

Durham Research Online

Deposited in DRO:

09 September 2014

Version of attached file:

Published Version

Peer-review status of attached file:

Peer-reviewed

Citation for published item:

King, J.A. and Ganguly, A. and Burn, D.M. and Pal, S. and Sallabank, E.A. and Hase, T.P.A. and Hindmarch, A.T. and Barman, A. and Atkinson, D. (2014) 'Local control of magnetic damping in ferromagnetic/non-magnetic bilayers by interfacial intermixing induced by focused ion-beam irradiation.', *Applied physics letters.*, 104 (24). p. 242410.

Further information on publisher's website:

<http://dx.doi.org/10.1063/1.4883860>

Publisher's copyright statement:

© 2014 American Institute of Physics. This article may be downloaded for personal use only. Any other use requires prior permission of the author and the American Institute of Physics. The following article appeared in *Applied Physics Letters* 104, 242410 (2014) and may be found at <http://dx.doi.org/10.1063/1.4883860>

Additional information:

Use policy

The full-text may be used and/or reproduced, and given to third parties in any format or medium, without prior permission or charge, for personal research or study, educational, or not-for-profit purposes provided that:

- a full bibliographic reference is made to the original source
- a [link](#) is made to the metadata record in DRO
- the full-text is not changed in any way

The full-text must not be sold in any format or medium without the formal permission of the copyright holders.

Please consult the [full DRO policy](#) for further details.

Local control of magnetic damping in ferromagnetic/non-magnetic bilayers by interfacial intermixing induced by focused ion-beam irradiation

J. A. King, A. Ganguly, D. M. Burn, S. Pal, E. A. Sallabank, T. P. A. Hase, A. T. Hindmarch, A. Barman, and D. Atkinson

Citation: [Applied Physics Letters](#) **104**, 242410 (2014); doi: 10.1063/1.4883860

View online: <http://dx.doi.org/10.1063/1.4883860>

View Table of Contents: <http://scitation.aip.org/content/aip/journal/apl/104/24?ver=pdfcov>

Published by the [AIP Publishing](#)

Articles you may be interested in

[Magnetic strip patterns induced by focused ion beam irradiation](#)

J. Appl. Phys. **103**, 063915 (2008); 10.1063/1.2894587

[Resolution in focused electron- and ion-beam induced processing](#)

J. Vac. Sci. Technol. B **25**, 2219 (2007); 10.1116/1.2789441

[Determination and reduction of ion-beam etching induced magnetic dead layer](#)

J. Appl. Phys. **97**, 10N901 (2005); 10.1063/1.1851871

[Aberration properties of focused ionbeam induced by space charge effect](#)

J. Vac. Sci. Technol. B **10**, 2814 (1992); 10.1116/1.586008

[Focused ionbeam crater arrays for induced nucleation of diamond film](#)

J. Vac. Sci. Technol. B **7**, 1947 (1989); 10.1116/1.584653



Free online magazine

**MULTIPHYSICS
SIMULATION**

[READ NOW ▶](#)

The COMSOL logo consists of a small red square followed by the word 'COMSOL' in a bold, sans-serif font.

Local control of magnetic damping in ferromagnetic/non-magnetic bilayers by interfacial intermixing induced by focused ion-beam irradiation

J. A. King,^{1,a)} A. Ganguly,^{2,a)} D. M. Burn,¹ S. Pal,² E. A. Sallabank,¹ T. P. A. Hase,³ A. T. Hindmarch,¹ A. Barman,^{2,b)} and D. Atkinson^{1,b)}

¹Department of Physics, Durham University, Durham DH1 3LE, United Kingdom

²Thematic Unit of Excellence on Nanodevice Technology and Department of Condensed Matter Physics and Material Sciences, S.N. Bose National Centre for Basic Sciences, Salt Lake, Kolkata 700 098, India

³Department of Physics, University of Warwick, Coventry CV4 7AL, United Kingdom

(Received 28 February 2014; accepted 4 June 2014; published online 18 June 2014)

The influence of interfacial intermixing on the picosecond magnetization dynamics of ferromagnetic/non-magnetic thin-film bilayers was studied. Low-dose focused-ion-beam irradiation was used to induce intermixing across the interface between a 10 nm Ni₈₁Fe₁₉ layer and a 2–3 nm capping layer of either Au or Cr. Time-resolved magneto-optical Kerr effect was used to study magnetization dynamics as a function of ion-beam dose. With an Au cap, the damping of the un-irradiated bilayer was comparable with native Ni₈₁Fe₁₉ and increased with increasing ion dose. In contrast, for Ni₈₁Fe₁₉/Cr the damping was higher than that for native Ni₈₁Fe₁₉, but the damping decreased with increasing dose. © 2014 AIP Publishing LLC.

[<http://dx.doi.org/10.1063/1.4883860>]

Picosecond magnetization dynamics are largely controlled by damped precessional processes, and consequently, magnetic damping has received significant research attention both for the fundamental physics involved¹ and for technological applications.² For spin-transfer torque magnetic random access memory (STT-MRAM) and magnonic devices, low damping facilitates a lower writing current and longer propagation of spin waves; higher damping is desirable for increasing the reversal rates and the coherent reversal of magnetic elements, as damping suppresses the precessional motion of the magnetization vector. In general, the control of magnetic properties at the micro- and nano-scale is important for technological applications.

Magnetization dynamics are commonly described phenomenologically by the Landau-Lifshitz-Gilbert equation³

$$\frac{d\mathbf{M}}{dt} = -\gamma\mathbf{M} \times \mathbf{H}_{eff} + \frac{\alpha}{M_s}\mathbf{M} \times \frac{d\mathbf{M}}{dt}, \quad (1)$$

where \mathbf{M} is the magnetization, γ is the gyromagnetic ratio, \mathbf{H}_{eff} is the effective magnetic field, and α is the dimensionless Gilbert damping coefficient. The damping coefficient can be modified by introducing doping elements including rare earths^{4–7} or transition metal^{8,9} elements, with the dopant introduced by co-deposition, usually co-sputtering. A disadvantage of this approach is that the entire material is doped.

An alternative method for doping is direct irradiation with an ion beam of the desired dopant.¹⁰ Dopants including Cr,¹⁰ Tb,¹¹ Gd,¹¹ Ni,¹² and Fe¹³ have been introduced as implanted ions. This approach can be used to introduce dopants into a localized area via lithography,^{11,14} with an appropriate ion source. High-energy beams are needed to ensure adequate doping, requiring either a research accelerator or a

commercially available accelerator-based ion implanter.¹¹ High-energy heavy-ion irradiation is not usually compatible with local patterning.¹⁵

Dopants introduced by ion-irradiation can affect the magnetic properties by introducing specific atomic species into the material, by altering the microstructure of the magnetic material (e.g., recrystallization or amorphization) or through intermixing in multilayered structures. The saturation magnetization, magnetic anisotropy, coercivity, and damping can be modified by direct ion implantation.^{12,16} Sufficient dopant can be introduced to produce significant alterations to the magnetic behavior, for example, irradiation by Cr⁺ ions can cause paramagnetism in NiFe¹⁶ and both Tb⁺ and Gd⁺ ions modify the damping in NiFe. These results are similar to those obtained from co-sputtering, thus indicating the effects are intrinsic to the dopants.¹¹ However, in the case of Cr, the damping varies according to whether the Cr is co-sputtered or ion-implanted,¹⁰ with the biggest increase observed for implantation. With the exception of recent work on epitaxial vanadium-doped iron,¹⁷ the addition of dopants typically increases damping.⁸ Spin-wave waveguides have recently been fabricated by implanting Cr ions in selective areas of NiFe by lithographic patterning.¹⁴ Ion beam irradiation can also modify the magnetic behavior through direct modification of the structure of the material being irradiated, without the ions acting as a dopant. Ion bombardment of a solid interface results in thousands of intermixed atoms per single ion impact.²¹ Ar⁺ ion irradiation has been shown to cause intermixing in Co/Pt layers, grain growth and increased interfacial roughening, changing the magnetization from perpendicular to in-plane,¹⁸ while intermixing in antiferromagnetic/ferromagnetic bilayers has been shown to modify the damping.¹⁹ Also, light ions, such as He⁺, can cause intermixing, but have been shown to end up buried in the substrate.²⁰ Local ion-beam-induced variations of magnetic properties have been introduced through resist-based lithographic techniques resulting in purely magnetic patterning.¹⁴

^{a)}J. A. King and A. Ganguly contributed equally to this work.

^{b)}Authors to whom correspondence should be addressed. Electronic addresses: del.atkinson@durham.ac.uk and abarman@bose.res.in

In contrast to mask-based ion beam patterning, focused-ion-beam (FIB) irradiation allows direct nanoscale patterning without additional lithographic processes. However, although a range of ion species can be incorporated into FIBs, most commercial systems are limited to Ga^+ ions. Earlier work suggested that direct implantation of Ga^+ at high fluences is the main mechanism for modifying the magnetic properties²² and that moderate fluences can tune the coercivity, saturation magnetization and anisotropy field in NiFe/Au bilayers.²³ In bilayered or multilayered ferromagnetic/nonmagnetic (FM/NM) systems, low-dose FIB irradiation could be used to induce interfacial doping providing a route to locally modify the magnetic properties without substantial structural changes or damage.

Here, the magnetic damping behavior of ferromagnetic/non-magnetic thin-film bilayers was investigated as a function of systematic intermixing of the bilayer interface induced by low-dose focused-ion-beam irradiation. The dynamic magnetization response was measured by time-resolved magneto-optic Kerr effect (TR-MOKE) microscopy. The results indicate that intermixing across the FM/NM interface, using FIB provides a mechanism for local control of the damping within the bilayer system that may open opportunities for magnetic device applications and for creating magnonic crystal structures.

Measurements were made on FM/NM bilayer microstructures where the FM layer was $\text{Ni}_{81}\text{Fe}_{19}$ (nominal) with a thickness of 10 nm and a thin NM cap (2–3 nm) of either Au or Cr. Arrays of $30\ \mu\text{m}$ diameter circular structures were patterned from the same bilayer, allowing many different FIB irradiation doses to be applied to the same bilayer. The areas of the circles were small enough to irradiate relatively quickly but easy to locate and large enough for measurements of the magnetization using the TR-MOKE, the scale of structures also suggests any side-wall oxidation can be ignored.

The bilayers were deposited on to a hydrothermally oxidized Si/SiO₂ substrate by thermal evaporation, with the deposition of the NiFe, Au, and Cr from a base pressure of 1×10^{-7} Torr. Irradiation was performed using a FEI Helios Nanolab 600 FIB microscope with a 30 keV Ga^+ ion beam at normal incidence. The circles were individually irradiated by rastering the focused ion beam over a $50\ \mu\text{m}$ square area. Irradiation doses ranged from 0 to $2.5 \times 10^{15}\ \text{Ga}^+/\text{cm}^2$ (0–4 pC/ μm^2), using a beam current of 28 pA. This current should not result in significant heating and earlier work showed that the modifications depend on the total dose and not the specific current.²⁴

The dynamic magnetization behavior of individual lithographic structures was measured using an all-optical TR-MOKE system based upon a collinear two-color pump-probe geometry.²⁵ Magnetization was pumped with femtosecond laser pulses at a wavelength of 400 nm, a pulse width of 100 fs, and a typical fluence of $10\ \text{mJ}/\text{cm}^2$ (spot size of about $1\ \mu\text{m}$). The magnetization was probed with linearly polarized 800 nm wavelength pulses, with a 70 fs pulse width, and a typical fluence of $1.5\ \text{mJ}/\text{cm}^2$ (spot size 800 nm). A biasing magnetic field was applied at a small angle (5° – 15°) to the sample plane during the measurements, the in-plane component of which is referred to here as H .

The raw TR-MOKE data can be divided into three temporal regimes. First, an ultrafast demagnetization was observed within the first 500 fs, this was followed by a rapid remagnetization within 10 ps and a slower remagnetization (260 ps for NiFe/Au and 1.2 ns for NiFe/Cr), superimposed on which was damped oscillatory behavior. This oscillatory behavior represents the precessional motion of the magnetization. For analysis of the data, a bi-exponential background was fitted to the decaying signal and subtracted to isolate the precessional behavior. A fast Fourier transform with a Welch window function was used to obtain the frequency spectra. The time-domain data were fitted with an exponentially damped harmonic function to obtain the relaxation time and from this the damping coefficient α .²⁶

Figure 1 shows examples of the background-corrected magnetization oscillations measured for the NiFe/Au bilayer system as a function of low to moderate irradiation dose at $H = 1.5\ \text{kOe}$. In all cases, the data show damped single frequency sinusoidal behavior, allowing the evolution of α and the precessional frequency to be determined as a function of FIB dose, see Figure 2. For the un-irradiated bilayer α is approximately 0.01, which is consistent with the typical values for $\text{Ni}_{80}\text{Fe}_{20}$.²⁷ With increasing dose α increases, the data show some scatter but, to a first approximation, across the range investigated α increases linearly with dose at a rate of $0.0035\ \mu\text{m}^2/\text{pC}$. In contrast, the precessional frequency data show less scatter and are characterized by a general decrease upon which a small peak is imposed between 1.3 and $2.0\ \text{pC}/\mu\text{m}^2$.

Figure 3 shows examples of the background-corrected magnetization oscillations measured for the NiFe/Cr bilayer system as a function of low dose irradiation at $H = 1.5\ \text{kOe}$. Since the mass of Cr is lower than the Au the irradiation induced intermixing was expected to occur at lower doses, hence a smaller dose range was investigated. The damping coefficient α and the precessional frequencies for the NiFe/Cr bilayers are shown as a function of ion dose in Figure 4. In contrast to the NiFe/Au, the value of α of the un-irradiated NiFe/Cr bilayer was significantly higher than that for the uncapped NiFe, indicating an enhancement of the damping associated with the Cr layer. With increasing

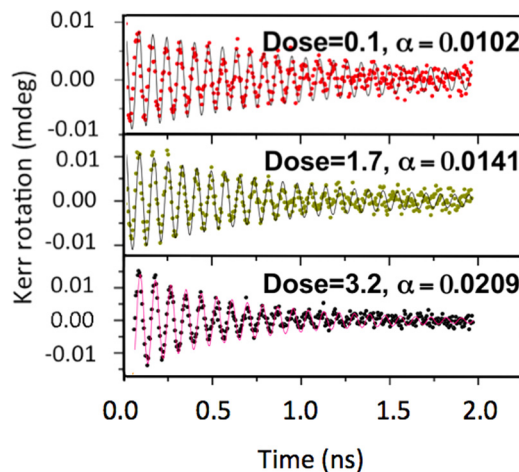


FIG. 1. Examples of the background-corrected magnetization oscillations measured using TR-MOKE for NiFe/Au bilayered microstructures as a function of low-to-moderate Ga^+ ion irradiation dose at $H = 1.5\ \text{kOe}$.

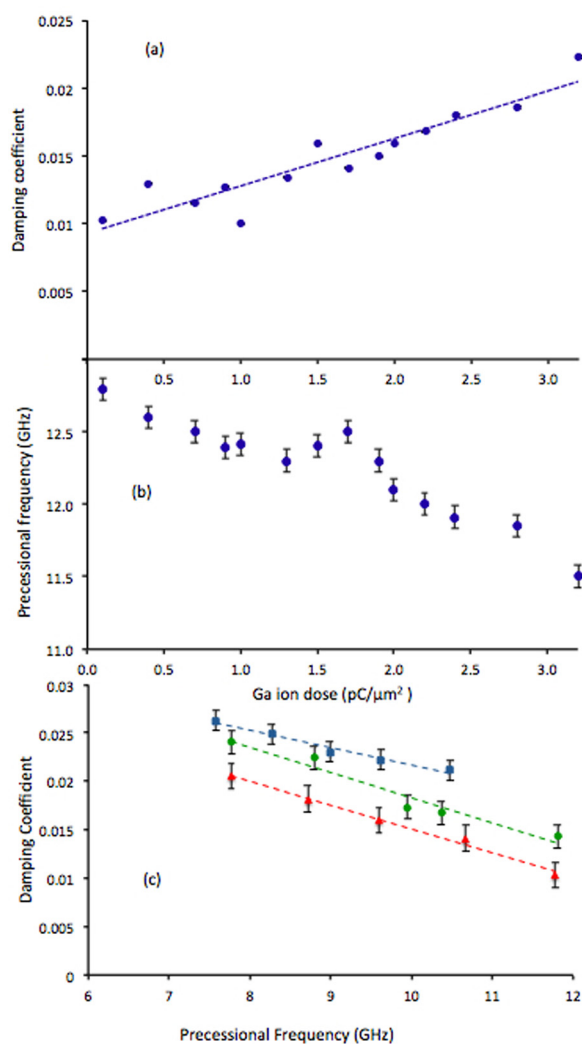


FIG. 2. (a) The damping coefficient, α , (note: error bars are smaller than data points) and (b) the precessional frequencies obtained from the TR-MOKE data of a NiFe/Au bilayer as a function of FIB dose at $H = 1.5$ kOe. (c) The precessional frequency dependence of the damping determined by varying H , for irradiation doses of 0.1 (triangle), 1.7 (circle), and 3.2 (square) pC/μm².

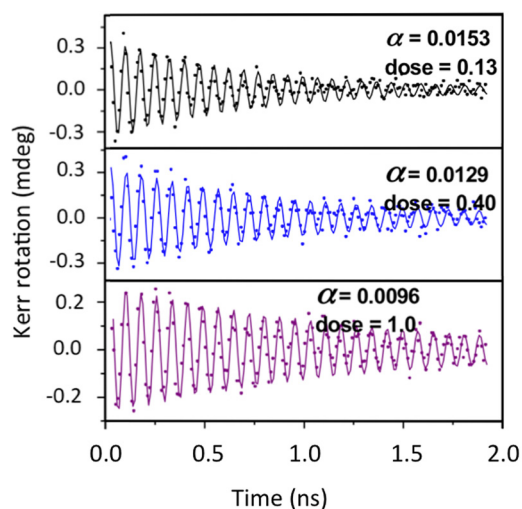


FIG. 3. Examples of the background-corrected magnetization oscillations measured for NiFe/Cr microstructures as a function of low Ga⁺ ion irradiation dose at $H = 1.5$ kOe.

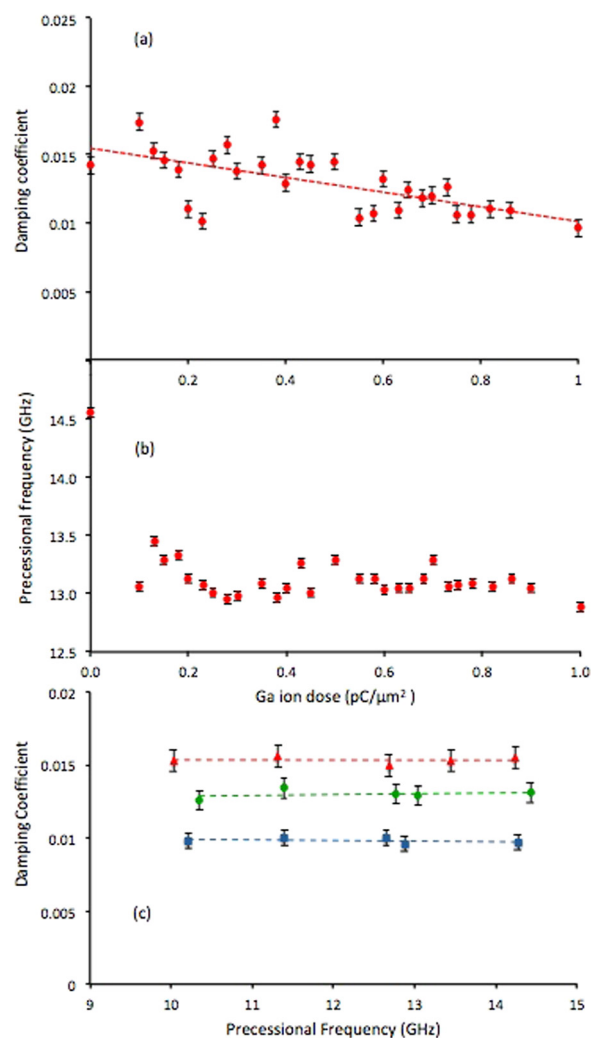


FIG. 4. (a) The damping coefficient, α , and (b) the precessional frequencies obtained from the TR-MOKE data of a NiFe/Cr bilayer as a function of FIB dose at $H = 1.5$ kOe. (c) The precessional frequency dependence of the damping determined by varying H , for irradiation doses of 0.13 (triangle), 0.40 (circle), and 1.00 (square) pC/μm².

dose, the damping showed significant variability but, in general, fell at a rate of $0.0054 \mu\text{m}^2/\text{pC}$.

Detailed analysis of the structural changes induced by low-dose FIB irradiation in NiFe/Au bilayers, undertaken using grazing incidence x-ray reflectivity, x-ray fluorescence, and Monte Carlo simulations,²⁸ showed that sputtering of material was very limited at these doses and restricted to the non-magnetic capping layer. Also, Ga⁺ implantation was a very small dopant fraction (up to the order of 1%) over the relevant dose range. In contrast, intermixing at the FM/NM interface was significant, leading to a compositionally graded alloy extending over several nanometers at the interface.²⁸ Furthermore, quasi-static MOKE, SQUID, and x-ray magnetic circular dichroism (XMCD) measurements of FIB irradiated NiFe/Au bilayers revealed complex changes in the magnetization as a function of the ion beam dose.²⁴ For a 2.5 nm Au cap, the saturation magnetization falls rapidly in the low dose regime to a minimum around 1.3–2.0 pC/μm² and recovers to a small peak before falling further with increasing irradiation.²⁴

There have been significant developments in the theoretical understanding of the mechanisms for damping in

Fe,^{29–31} Ni,^{29–31} and Co^{30,31} and more generally in transition metal alloys (NiFe),²⁷ which have shown the significance of the effective field from spin-orbit coupling and of scattering processes. Spin-pumping across interfaces and two-magnon mediated processes in FM/NM films have also been identified as possible mechanisms for enhanced damping.^{32–35} Following Woltersdorf *et al.*,³⁵ additional measurements were undertaken here on selected samples at different magnetic fields over range of 1.3–0.8 kOe for NiFe/Au and 1.7–0.9 kOe for NiFe/Cr to vary the precessional frequency and shed light on the damping mechanism, see Figures 2(c) and 4(c).

Here, the damping parameter for the un-irradiated Au capped NiFe was comparable with that of uncapped NiFe, suggesting insignificant spin-pumping effects. Ion-beam irradiation increases the precessional damping, which is associated with a broadening of the interfacial zone by intermixing between the NiFe and Au. This compositionally graded NiFeAu alloy extends over a few nanometers at the interface and may increase the damping by enhanced scattering and/or modification of the spin-orbit interaction. The field-dependent damping of the NiFe/Au was observed to decrease steadily with increasing frequency, indicating an extrinsic two-magnon type contribution to the damping that may be associated with increased disorder. This contrasts with the behavior observed for MBE grown Au on Fe, where the damping was enhanced by spin-pumping effects.³⁵ Enhanced scattering is expected to increase the electrical resistivity³⁶ and this was observed for the NiFe/Au bilayer.²⁴ The precessional frequency falls with ion beam dose, but displays a small peak that is correlated in dose with a feature in the dose dependent magnetic moment.²⁸ The origin of this behavior is not currently understood.

Capping NiFe with Cr increased the α value by $\sim 50\%$ compared to uncapped NiFe. With increasing ion dose, the damping coefficient was reduced, falling to 0.0096 at the maximum dose, which is comparable with uncapped NiFe. The enhanced damping compared to uncapped NiFe could be an intrinsic effect associated with spin pumping across the interface or d - d hybridization of the Fe and Cr at the interface that increases the d -band width of the NiFe in contact with the Cr layer, modifying the spin-orbit interaction. Alternatively, the increased damping could result from extrinsic two-magnon scattering linked to the coupling across the interface. However, the damping of NiFe/Cr was invariant with increasing precessional frequency for the doses investigated. This indicates an enhancement of the intrinsic damping, which contrasts with the effect of Cr on Fe observed for MBE grown samples³⁵ that identified an extrinsic two-magnon scattering contribution to the damping. Here, the enhancement may be associated with the thickness of the Cr layer or the interfacial structure. Both are modified by ion-beam irradiation, with the loss of some Cr from the surface by sputtering and increased interfacial intermixing, which could disrupt this spin-pumping or interface hybridization, respectively, thereby reducing the damping, ultimately towards to a single NiFe layer value. The precessional frequency of the Cr capped NiFe fell sharply with the lowest irradiation dose and changed little with further irradiation. This may also result from interfacial

hybridization that increases the NiFe moment and hence the precessional frequency of the un-irradiated sample. Subsequent irradiation may degrade the moment and the precessional frequency would fall.

In summary, low-dose focused Ga⁺ ion beam irradiation of ferromagnetic/non-magnetic thin-film bilayers has demonstrated that the precessional magnetization behavior can be effectively tuned. For NiFe with a Au capping layer, the damping coefficient of the un-irradiated bilayer was comparable with that of native NiFe, and the damping parameter increased with increasing ion beam dose. In contrast, capping NiFe with Cr increased the damping parameter compared to the native NiFe, and the damping parameter then decreased with increasing ion beam irradiation dose. The combination of the low doses coupled with the high spatial resolution of the focused-ion-beam suggests this methodology may be applicable for locally modifying the precessional magnetization behavior of ferromagnetic materials with feature sizes down to the nanoscale. This methodology may have application to local control of damping for magnetic and spintronic device applications.

We gratefully acknowledge financial support from Department of Science and Technology, Government of India, and the British Council for the DST-UKIERI joint project, Grant No. DST/INT/UK/P-44/2012. D.A. also acknowledges EPSRC funding (EP/G010897/1 and Durham Strategic Partnership Award) and UK CRG XMaS beam-line at ESRF.

¹P. S. Keatley, V. V. Kruglyak, P. Gangmei, and R. J. Hicken, *Philos. Trans. R. Soc. A* **369**, 3115 (2011).

²C. H. Marrows and B. J. Hickey, *Philos. Trans. R. Soc. A* **369**, 3027 (2011).

³T. Gilbert, *IEEE Trans. Magn.* **40**, 3443 (2004).

⁴W. Bailey, P. Kabos, F. Mancoff, and S. Russek, *IEEE Trans. Magn.* **37**, 1749 (2001).

⁵T. A. Moore, P. Mohrke, L. Heyne, A. Kaldun, M. Klaui, D. Backes, J. Rhensius, L. J. Heyderman, J.-U. Thiele, G. Woltersdorf *et al.*, *Phys. Rev. B* **82**, 094445 (2010).

⁶S. G. Reidy, L. Cheng, and W. E. Bailey, *Appl. Phys. Lett.* **82**, 1254 (2003).

⁷G. Woltersdorf, M. Kiessling, G. Meyer, J. U. Thiele, and C. H. Back, *Phys. Rev. Lett.* **102**, 257602 (2009).

⁸J. O. Rantschler, R. D. McMichael, A. Catillo, A. J. Shapiro, W. F. Egelhoff, Jr., B. B. Maranville, D. Pulugurtha, A. P. Chen, and L. M. Connors, *J. Appl. Phys.* **101**, 033911 (2007).

⁹S. Ingvarsson, X. Gang, S. S. P. Parkin, and R. H. Koch, *Appl. Phys. Lett.* **85**, 4995 (2004).

¹⁰J. Fassbender, J. von Borany, A. Mücklich, K. Potzger, W. Möller, J. McCord, L. Schultz, and R. Mattheis, *Phys. Rev. B* **73**, 184410 (2006).

¹¹V. Dasgupta, N. Litombe, and W. E. Bailey, *J. Appl. Phys.* **99**, 08G312 (2006).

¹²J. Fassbender and J. McCord, *Appl. Phys. Lett.* **88**, 252501 (2006).

¹³D. G. Park, K. C. Heo, W. W. Kim, and Y. M. Choong, *Phys. Status Solidi* **4**, 4577 (2007).

¹⁴B. Obray, T. Meyer, P. Pirro, T. Bracher, B. Lagel, J. Osten, T. Strache, J. Fassbender, and B. Hillebrands, *Appl. Phys. Lett.* **102**, 022409 (2013).

¹⁵J. Fassbender and J. McCord, *J. Magn. Magn. Mater.* **320**, 579 (2008).

¹⁶L. Folks, R. E. Fontana, B. A. Gurney, J. R. Childress, S. Maat, J. A. Katine, J. E. E. Baglin, and A. J. Kellock, *J. Phys. D: Appl. Phys.* **36**, 2601 (2003).

¹⁷C. Scheck, L. Cheng, I. Barsukov, Z. Frait, and W. E. Bailey, *Phys. Rev. Lett.* **98**, 117601 (2007).

¹⁸M. J. Bonder, N. D. Telling, P. J. Grundy, C. A. Fauce, T. Shen, and V. M. Vishnyakov, *J. Appl. Phys.* **93**, 7226 (2003).

¹⁹J. McCord, T. Strache, I. Monch, R. Mattheis, and J. Fassbender, *Phys. Rev. B* **83**, 224407 (2011).

- ²⁰J. Fassbender, D. Ravelosona, and Y. Samson, *J. Phys. D: Appl. Phys.* **37**, R179 (2004).
- ²¹W. Bolse, *Mater. Sci. Eng., A* **253**, 194 (1998).
- ²²W. M. Kaminsky, G. A. C. Jones, N. K. Patel, W. E. Booij, M. G. Blamire, S. M. Gardiner, Y. B. Xu, and J. A. C. Bland, *Appl. Phys. Lett.* **78**, 1589 (2001).
- ²³C. C. Faulkner, D. Atkinson, D. A. Allwood, and R. P. Cowburn, *J. Magn. Mater.* **319**, 9 (2007).
- ²⁴D. M. Burn Ph.D. Thesis, Durham University (2013); D. M. Burn, T. P. A. Hase, and D. Atkinson, *J. Phys.: Condens. Matter* **26**, 236002 (2014).
- ²⁵S. Pal, B. Rana, O. Hellwig, T. Thomson, and A. Barman, *Appl. Phys. Lett.* **98**, 082501 (2011).
- ²⁶A. Barman S. Wang, J. Maas, A. R. Hawkins, S. Kwon, J. Bokor, A. Liddle, and H. Schmidt, *Appl. Phys. Lett.* **90**, 202504 (2007).
- ²⁷A. A. Starikov, P. J. Kelly, A. Brataas, Y. Tserkovnyak, and G. E. W. Bauer, *Phys. Rev. Lett.* **105**, 236601 (2010).
- ²⁸E. Arac, D. M. Burn, D. S. Eastwood, T. P. Hase, and D. Atkinson, *J. Appl. Phys.* **111**, 044324 (2012).
- ²⁹V. Kambersky, *Phys. Rev. B* **76**, 134416 (2007).
- ³⁰K. Gilmore, Y. U. Idzerda, and M. D. Stiles, *Phys. Rev. Lett.* **99**, 027204 (2007).
- ³¹K. Gilmore, Y. U. Idzerda, and M. D. Stiles, *J. Appl. Phys.* **103**, 07D303 (2008).
- ³²R. Urban, G. Woltersdorf, and B. Heinrich, *Phys. Rev. Lett.* **87**, 217204 (2001).
- ³³Y. Tserkovnyak and A. Brataas, *Phys. Rev. Lett.* **88**, 117601 (2002).
- ³⁴Th. Gerrits, M. L. Schneider, and T. J. Silva, *J. Appl. Phys.* **99**, 023901 (2006).
- ³⁵G. Woltersdorf, M. Buess, B. Heinrich, and C. H. Back, *Phys. Rev. Lett.* **95**, 037401 (2005).
- ³⁶S. Ingvarsson, L. Ritchie, X. Y. Liu, G. Xiao, J. C. Slonczewski, P. L. Trouilloud, and R. H. Koch, *Phys. Rev. B* **66**, 214416 (2002).